

Computer Simulations of the Solvent Dependence of Apolar Association Strength: Gibbs Free Energy Calculations on a Cyclophane–Pyrene Complex in Water and Chloroform

Tiziana Z. Mordasini Denti,[†] Wilfred F. van Gunsteren,^{*,‡} and François Diederich^{*,†}

Contribution from the Laboratorium für Organische Chemie and Laboratorium für Physikalische Chemie, Eidgenössische Technische Hochschule, 8092 Zürich, Switzerland

Received February 8, 1996. Revised Manuscript Received April 27, 1996[⊗]

Abstract: The inclusion complexation of pyrene with the macrobicyclic cyclophane host **1** has been described in previous experimental studies and showed a strong solvent dependence. Upon changing from apolar to dipolar aprotic, to polar protic solvents, and to water, the association strength of complex **2** increases steadily. Following a detailed conformational analysis of this system, we then performed Gibbs free energy calculations using molecular dynamics (MD) simulations in the liquid phase. The purpose of this work was to test the reproducibility of the experimental results with computer simulation techniques and obtain more details at the molecular level on the origin of these strong solvent effects. Gibbs free energy calculations of cyclophane–pyrene complex **2** in water and in chloroform were carried out by performing a deletion of the pyrene molecule in the pure solvent and inside the cyclophane cavity, following the double annihilation technique. The procedure allowed the free energy of complexation in both solvents to be obtained. The scaling of the nonbonded potential energy functions was performed using a soft-core interaction function. The result confirmed the experimentally measured trend of a stronger complexation in water than in chloroform ($\Delta(\Delta G)_{\text{exp}} = 7.1 \text{ kcal mol}^{-1}$, $T = 303 \text{ K}$). Although the absolute value was overestimated ($\Delta(\Delta G)_{\text{calc}} = 10.2 \text{ kcal mol}^{-1}$), the result confirms the efficiency of the soft-core scaling technique for the deletion of large molecules. Moreover, it could be shown that in this case the strong solvent dependence of the cyclophane–pyrene complexation is mainly due to the different free energies of cavitation in water and chloroform. The stronger cohesive interactions of water make the disappearance of pyrene from the solution into the cyclophane cavity more favorable than in chloroform.

1. Introduction

Molecular complexation is the basis for most biological processes,¹ and it is of great interest to obtain a profound understanding of the mechanisms, which govern the recognition between molecules. Apolar complexation is strongest in aqueous solution^{2,3} and provides the major driving force for almost all types of biological recognition processes such as enzyme–substrate complexation, protein folding, and membrane aggregation. Due to the complexity of biological systems, molecular level information on apolar biological complexation processes is best obtained in experimental and theoretical studies on suitable model systems.⁴ Some time ago we became interested in investigating the role of solvent in apolar complexation and were fortunate to develop a receptor, cyclophane **1**,⁵ which displayed solubility in solvents of all polarity. The binding ability of this receptor could be studied in a great variety of environments, mimicking both the highly polar biological aqueous phases as well as the less polar lipidic membranes. By a combination of methods including microcalorimetry, ¹H-NMR,

UV/vis, and fluorescence titrations, we determined the thermodynamic characteristics ΔG and, in most cases, also ΔH and $T\Delta S$ for the formation of cyclophane–pyrene complex **2** in solvents of different polarity, extending from water to carbon disulfide.² A dramatic solvent dependence was obtained: upon changing from water, the most polar, to chloroform, an apolar solvent, the complexation free energies at 303 K decreased from $-\Delta G = 9.4$ to $2.3 \text{ kcal mol}^{-1}$, resulting in a difference in complexation free energy of $7.1 \text{ kcal mol}^{-1}$ (Table 1). In order to generate a better understanding of this large difference in association strength, we decided to use computer simulations of atomistic molecular models and Gibbs free energy calculations using these models.^{4,6} Free energy calculations based on molecular simulation have been widely applied in the past decade and were proven to be very powerful for solving chemical and biochemical problems, going from calculations on binding affinity for host–guest systems,^{4,7–10} to protein–inhibitor interactions,^{11–14} to studies on simple model systems.^{15–17} There is no X-ray crystal structure available for complex **2**, but

[†] Laboratorium für Organische Chemie.

[‡] Laboratorium für Physikalische Chemie.

[⊗] Abstract published in *Advance ACS Abstracts*, June 1, 1996.

(1) Sammes, P. G.; Taylor, J. B., Eds. *Comprehensive Medicinal Chemistry*; Ramsden, C. A., Volume Ed.; Pergamon Press: Oxford, 1990; Vol. 4.

(2) Smithrud, D. B.; Diederich, F. *J. Am. Chem. Soc.* **1990**, *112*, 339–343.

(3) Smithrud, D. B.; Wyman, T. B.; Diederich, F. *J. Am. Chem. Soc.* **1991**, *113*, 5420–5426.

(4) Jorgensen, W. L.; Nguyen, T. B.; Sanford, E. M.; Chao, I.; Houk, K. N.; Diederich, F. *J. Am. Chem. Soc.* **1992**, *114*, 4003–4004.

(5) Diederich, F.; Dick, K.; Griebel, D. *J. Am. Chem. Soc.* **1986**, *108*, 2273–2286.

(6) Jorgensen, W. L. *Acc. Chem. Res.* **1989**, *22*, 184–189.

(7) Lybrand, T. P.; McCammon, J. A.; Wipff, G. *Proc. Natl. Acad. Sci. U.S.A.* **1986**, *83*, 833–835.

(8) Grootenhuis, P. D. J.; Kollman, P. A. *J. Am. Chem. Soc.* **1989**, *111*, 2152–2158.

(9) Miyamoto, S.; Kollman, P. A. *J. Am. Chem. Soc.* **1992**, *114*, 3668–3694.

(10) Roux, B.; Karplus, M. *Biophys. J.* **1991**, *59*, 961–981.

(11) Merz, K. M.; Kollman, P. A. *J. Am. Chem. Soc.* **1989**, *111*, 5649–5658.

(12) Wong, C. F.; McCammon, J. A. *J. Am. Chem. Soc.* **1986**, *108*, 3830–3832.

(13) Rao, B. G.; Singh, U. C. *J. Am. Chem. Soc.* **1991**, *113*, 6735–6750.

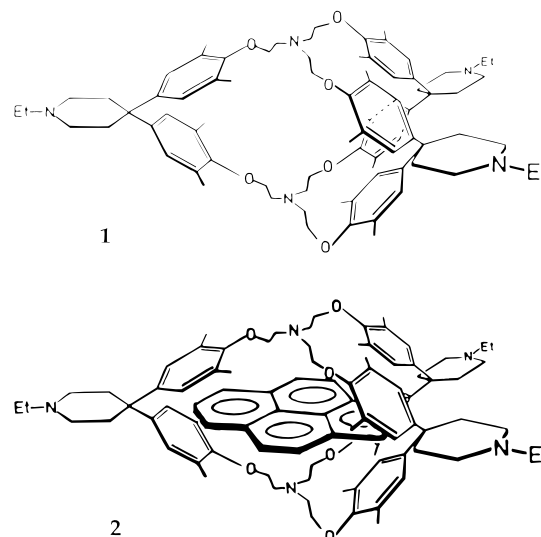
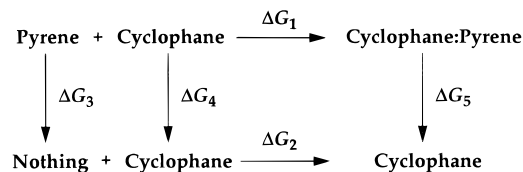
Table 1. Association Constants K_a (L mol⁻¹) and Free Energies of Formation $-\Delta G^\circ$ (kcal mol⁻¹) for Complex **2** in Eighteen Solvents of Different Polarity As Expressed by $E_T(30)^{44}$ Values (kcal mol⁻¹) at $T = 303$ K²

run no.	solvent	K_a	$-\Delta G^\circ$	$E_T(30)$
1	water/1% Me ₂ SO ^a	6.0×10^6	9.4	63.0
2	2,2,2-trifluoroethanol/1% Me ₂ SO	4.2×10^5	7.8	59.4
3	ethylene glycol/10% Me ₂ SO	1.8×10^5	7.3	55.9
4	methanol	4.4×10^4	6.4	55.5
5	formamide/10% Me ₂ SO	3.0×10^4	6.2	55.2
6	ethanol	2.5×10^4	6.1	51.9
7	<i>N</i> -methylacetamide/10% Me ₂ SO	1.5×10^4	5.8	52.1
8	<i>N</i> -methylformamide/10% Me ₂ SO	4.8×10^3	5.1	54.0
9	acetone	1.2×10^3	4.3	42.2
10	<i>N,N</i> -dimethylacetamide/10% Me ₂ SO- <i>d</i> ₆	1.1×10^3	4.2	43.0
11	dimethyl sulfoxide- <i>d</i> ₆ ^b	6.9×10^2	3.9	45.0
12	<i>N,N</i> -dimethylformamide- <i>d</i> ₇ /10% Me ₂ SO- <i>d</i> ₆	1.6×10^2	3.0	43.7
13	<i>N,N</i> -dimethylformamide- <i>d</i> ₇	1.5×10^2	2.9	43.8
14	dichloromethane- <i>d</i> ₂	1.2×10^2	2.9	41.4
15	tetrahydrofuran- <i>d</i> ₈	8.4×10^1	2.7	37.4
16	chloroform- <i>d</i> ₁	4.3×10^1	2.3	39.1
17	benzene- <i>d</i> ₆	1.2×10^1	1.5	34.5
18	carbon disulfide	9×10^0	1.3	32.6

^a The aqueous solution contains $[\text{Na}_2\text{CO}_3] = 10^{-3}$ mol L⁻¹ to prevent protonation of the pentaamine host. ^b H/D solvent isotope effects are below the error in K_a which is $\pm 20\%$.

the complexation-induced changes in chemical shift observed during the ¹H-NMR binding titrations for as many as 10 different host and guest resonances suggested the formation of a highly ordered, structured complex of similar geometry in both water and chloroform. After having carried out a conformational analysis of **2**,¹⁸ which nicely reproduced the geometry proposed based on the experimental NMR data, we now describe computer liquid phase simulations of the complex. The aim of this study was to first reproduce the experimentally measured complexation free energies in water and in chloroform, testing the computer simulation capabilities, and then reach a deeper understanding of the solvent effects at the origin of the large stability difference seen in the two environments of very different polarity. We hoped to demonstrate that such interplay between experiment and computer simulations⁴ could give useful insight into solvent effects in general.

In this article we present Gibbs free energy calculations on cyclophane–pyrene complex **2** using molecular dynamics (MD) simulations¹⁹ with thermodynamic integration²⁰ in water and in chloroform. Thermodynamic integration was performed along a recently developed pathway that uses a soft-core scaling²¹ of the nonbonded potential energy functions in order to avoid numerical singularities and instabilities. The double annihilation technique²² allowed for a calculation of the Gibbs free energy of complexation using two sets of simulations for each solvent (water and chloroform), according to the following thermodynamic cycle:

**Figure 1.** The uncomplexed cyclophane molecule (**1**) and the complex with a pyrene molecule (**2**).**Scheme 1.** Thermodynamic Cycle Used for the Calculation of the Free Energy of Complexation for the Cyclophane–Pyrene System in Water and in Chloroform

ΔG_1 corresponds to the experimentally measured free energy of complexation in water or in chloroform, depending on the solvent, in which the thermodynamic cycle is performed. A simulation of the real complexation process would require an initial configuration where host and guest are separately diffusing in a solvent box, and a final configuration with the guest complexed into the host cavity. However, the configurational space available to the guest is terribly large. This means that the probability of the guest finding the host and entering the cavity in the right orientation is very small, if compared to the number of configurations that are usually sampled in a reasonable simulation time. In theory, only an infinite simulation could sample the entire configurational space. Hence, in simulations one has to make approximations trying to generate a number of configurations that are representative for the total ensemble of configurations. A compromise must be found between computational time and precision of the results. A process such as host–guest complexation as it occurs in nature would therefore need a huge number of configurations in order to deliver a good approximation of the complexation free energy, leading to unacceptably large computational times. It is therefore easier, in terms of computation, to perform the two artificial deletions of the pyrene molecule first in a solvent box (ΔG_3) and then inside the cavity of the solvated cyclophane (ΔG_5). The free energies ΔG_2 and ΔG_4 do not contribute to the total free energy, since they correspond to a mutation from the cyclophane molecule to itself, for which ΔG is zero. Closing the cycle shows that the (experimentally measured) free energy of complexation can be obtained by calculating the difference in free energy between deleting the guest molecule in pure solvent and inside the cavity of the solvated cyclophane molecule (double annihilation²²), as expressed in eq 1:

$$\Delta G_1 = \Delta G_3 - \Delta G_5 \quad (1)$$

(14) Bash, P. A.; Singh, U. C.; Brown, F. K.; Langridge, R.; Kollman, P. A. *Science* **1987**, *235*, 574–576.

(15) Jorgensen, W. L.; Nguyen, T. B. *J. Comput. Chem.* **1993**, *14*, 195–205.

(16) Lee, F. S.; Chu, Z. T.; Warshel, A. *J. Comput. Chem.* **1993**, *14*, 161–185.

(17) Jorgensen, W. L.; Severance, D. L. *J. Am. Chem. Soc.* **1990**, *112*, 4768–4774.

(18) Mordasini Denti, T.; van Gunsteren, W. F.; Diederich, F. *Computational Approaches in Supramolecular Chemistry*; NATO ASI Series C 426; Wipff, G., Ed.; Kluwer: Dordrecht, 1994; pp 117–136.

(19) Alder, B. J.; Wainwright, T. E. *J. Chem. Phys.* **1957**, *27*, 1208–1209.

(20) Kirkwood, J. G. *J. Chem. Phys.* **1935**, *3*, 300–313.

(21) Beutler, T. C.; Mark, A. E.; van Schaik, R. C.; Gerber, P. R.; van Gunsteren, W. F. *Chem. Phys. Lett.* **1994**, *222*, 529–539.

(22) Jorgensen, W. L.; Buckner, J. K.; Boudon, S.; Tirado-Rives, J. *J. Chem. Phys.* **1988**, *89*, 3742–3746.

The cycle was separately carried out with water and with chloroform as solvent. The difference in free energy of complexation between the water and the chloroform processes ($\Delta G_{1,(\text{CHCl}_3)} - \Delta G_{1,(\text{H}_2\text{O})}$) should finally deliver a value in agreement with the experimentally measured value of 7.1 kcal mol⁻¹.

2. Theory and Methods

The exact calculation of free energy²³ using the statistical mechanical definition involves the evaluation of the partition function of the system. In terms of computer simulations, this would mean a sampling of the entire configurational space available to the system, which corresponds to an ideal infinite calculation. The problem has a solution if the entire ensemble of configurations is approximated with a set of configurations, which are representative for the ensemble when calculating a particular property. In this way, the simulation time is reduced to a reasonable size and the results are correct within a good approximation. The relevant configurational space is further reduced if the initial and final states of the free energy calculation do not differ significantly. The more similar the initial and final states are, the more precise or efficient the calculation can be, because a relatively small part of configurational space must be sampled. However, sometimes one would calculate free energy differences between rather different molecules. In this case it is advantageous if a number of more related intermediate states (existing or artificial) are defined. The sum of the free energy increments between the different intermediate states then delivers at the end the desired total free energy difference.

Usually a so-called coupling parameter λ is used to define intermediate states between the end points, which allows the conversion of a system A, described by the Hamiltonian H_A , into the system B, described by the Hamiltonian H_B . The difference in Gibbs free energy can then be calculated as the work required for such a change. As an example, consider the simplest way for this interconversion, which is a linear coupling scheme:

$$H(\vec{p}, \vec{r}, \lambda) = (1 - \lambda)H_A(\vec{p}, \vec{r}) + \lambda H_B(\vec{p}, \vec{r}) \quad (2)$$

where \vec{r} and \vec{p} respectively represent the positions and conjugate momenta of all the particles. The Hamiltonian becomes in this way a function of the λ parameter.

Theoretically the pathway chosen for the interconversion of system A into system B, or in other words which kind of function of λ is chosen for the Hamiltonian, should not influence the result of the free energy calculation, because free energy is a state function. However, in practice the choice of the pathway becomes a crucial decision, which can considerably influence the final result. This is especially the case where deletion or creation of atoms is required. It is well-known,^{24,21} that in most cases of deletion or creation of atoms the use of a linear coupling scheme causes singularities and numerical instabilities, which considerably affect the precision of the free energy calculation and which require extrapolation methods to circumvent the singularities.

All these problems are solved if the recently developed soft-core scaling²¹ is used. This kind of scaling must be applied to the nonbonded interaction functions, i.e. to the van der Waals and electrostatic interaction functions, in which particles that are disappearing or emerging are involved, without any kind of bond shrinking. Lennard-Jones and electrostatic interactions, which usually show a singularity at the core of the atom ($r_{ij} = 0$), are gradually scaled down to zero (for the case of an atom deletion), following a pathway such that the interaction energy in eq 3 approaches a finite value and not infinity as r_{ij} approaches zero. The form of the soft-core scaling is given in (3):

$$U_{ij} = \lambda^n 4\epsilon_{ij} \left(\frac{1}{\left(\alpha_{LJ}(1 - \lambda)^2 + \left(\frac{r_{ij}}{\sigma_{ij}} \right)^6 \right)^2} - \frac{1}{\alpha_{LJ}(1 - \lambda)^2 + \left(\frac{r_{ij}}{\sigma_{ij}} \right)^6} \right) + \frac{\lambda^n q_i q_j}{4\pi\epsilon_0\epsilon_r(\alpha_C(1 - \lambda)^2 + r_{ij}^2)^{1/2}} \quad (3)$$

α_{LJ} and α_C are positive parameters which determine the soft-core behavior of the potential energy terms. σ_{ij} and ϵ_{ij} are the parameters of Lennard-Jones potential energy terms that mimic the van der Waals interactions. q_i and q_j denote the charges on the interaction sites i and j , and r_{ij} denotes the distances between interaction sites. The factor $\epsilon_0\epsilon_r$ represents the dielectric permittivity of the medium.

There are several possibilities to calculate Gibbs free energy differences. One of them is the thermodynamic integration. The free energy difference between two systems A and B, ΔG_{BA} , can be expressed as follows:

$$\Delta G_{BA} = G(\lambda=\lambda_B) - G(\lambda=\lambda_A) = \int_{\lambda_A}^{\lambda_B} G'(\lambda) d\lambda \quad (4)$$

where $G'(\lambda)$ represents the first derivative of $G(\lambda)$.

It can be demonstrated²⁰ that

$$G'(\lambda) = \langle \partial H(\lambda) / \partial \lambda \rangle_\lambda \quad (5)$$

where the brackets $\langle \rangle_\lambda$ represent an ensemble average obtained using the Hamiltonian $H(\lambda)$.

Inserting eq 5 in eq 4, we obtain eq 6:

$$\Delta G_{BA} = \int_{\lambda_A}^{\lambda_B} \left\langle \frac{\partial H(\lambda)}{\partial \lambda} \right\rangle_\lambda d\lambda \quad (6)$$

which is the fundamental equation of the thermodynamic integration methods. In practice this method involves the evaluation of $\langle \partial H(\lambda) / \partial \lambda \rangle_\lambda$ at different λ -points between $\lambda_A = 0$ and $\lambda_B = 1$. The integration of the obtained curve will then deliver the Gibbs free energy difference between the two systems A and B.

3. Conformational Analysis

The absence of an X-ray crystal structure for cyclophane–pyrene complex **2** forced us to build arbitrary structures in order to have a starting point for the conformational analysis. The starting conformations were built using the molecular modeling system MacroModel V3.5X²⁵ and the OPLS* force field.²⁵ Three conformations of free cyclophane **1** were postulated at the beginning—*in-in*, *in-out*, and *out-out*—which differed from each other in the position of the lone pairs on the pivotal amine nitrogens: they either pointed into (*in*) or outside (*out*) the cavity. Energy minimization of the three cyclophane conformations in the complex with the pyrene guest showed that the *in-in* conformations were ~ 2 kcal mol⁻¹ more stable than the *in-out* conformations, and ~ 3 kcal mol⁻¹ more stable than the *out-out* conformations. Apparently, the *in-in* conformations of the cyclophane allow a better complexation of the flat pyrene molecule.

The conformational search, which was performed on complex **2** in vacuo applying the Systematic Pseudo Monte Carlo (SPMC) method²⁶ implemented in the program Batchmin V3.5, found 16 structures which were within 20 kJ mol⁻¹ from the energetic minimum.

A superimposition of these 16 conformers (Figure 2) showed that these geometries were quite similar to each other, confirming the first impression of a highly rigid complex. The core of the cyclophane, which complexes the guest, appeared to be

(23) For a review on free energy calculations, see: (a) King, P. M. In *Computer Simulation of Biomolecular Systems*; van Gunsteren, W. F., Weiner, P. K., Wilkinson, A. J., Eds.; Escom: Leiden, 1993; Vol. 2, pp 267–314. (b) Kollman, P. *Chem. Rev.* **1993**, *93*, 2395–2417.

(24) Cross, A. J. *Chem. Phys. Lett.* **1986**, *128*, 198–202.

(25) Still, W. C. *MacroModel V 3.5X*; Columbia University: New York.

(26) Goodman, J. M.; Still, W. C. *J. Comp. Chem.* **1991**, *12*, 1110–1117.



Figure 2. Superimposition of the 16 structures within 20 kJ mol⁻¹ from the global minimum found with a SPMC search. The pyrene molecule is omitted for clarity.

relatively fixed, whereas the three spiro piperidine rings outside the cavity were found to be more flexible.

Complex **2** was then further studied by the Molecular Dynamics (MD) technique using the GROMOS²⁷ (GRoningen MOlecular Simulation) program package. The analysis of the root-mean-square (rms) fluctuations of the atoms calculated over a trajectory of 105 ps at 300 K in vacuo confirmed the results of the SPMC search, since the largest rms fluctuations occurred in the three external piperidine rings, whereas the six O-CH₂-CH₂-N bridges showed only approximately half of the rms fluctuation of the piperidine rings.

The SPMC search also showed that for each of the 16 energetically favored complex geometries, there existed two nearly isoenergetic orientations of the pyrene guest in the plane defined by the three spiro-centers, which differed from each other by ca. 30° rotation (Figure 3). Here again the MD simulations confirmed the results of the SPMC search, showing that the pyrene molecule can rotate inside the cavity. A further analysis of the rotation revealed that the pyrene molecule “jumps” between specific orientations, which correspond to the two isoenergetic orientations found with the SPMC search. The analysis of the six Aryl-O-CH₂-CH₂-N bridges of **1** in the 16 final conformations of the SPMC search showed that the lone pairs of the ether oxygen atoms prefer pointing outward. The protons at the CH₂ units attached to the oxygen atoms prefer turning inside the cavity, whereas the protons at the N-CH₂ units turn outward. ¹H-NMR experiments at [**1**] = 2.0 mM L⁻¹ and [pyrene] = 20 mM L⁻¹ in methanol-*d*₄ (saturation binding) showed that the O-CH₂ protons are shifted upfield by Δδ = 2.14 ppm, whereas the N-CH₂ protons move upfield by only 0.85 ppm. This large difference clearly reveals that on average the aryl ether methylene group is oriented into the cavity against the enclosed pyrene ring, whereas the methylene groups attached to the pivotal amine nitrogens prefer a position at greater distance from the guest, possibly orienting outward of the cavity. Thus, the SPMC conformational analysis nicely reproduces the ¹H-NMR experimental data.

The energetically best conformation found with the SPMC search was then used for the successive free energy calculations with the MD technique.

(27) van Gunsteren, W. F.; Berendsen, H. J. C. *Groningen Molecular Simulations (GROMOS) Library Manual*; Biomos: Groningen, 1987.

4. Simulations

The simulations were carried out using the MD technique within the GROMOS²⁷ program package. The GROMOS force field was used combined with OPLS^{17,28} molecular force field parameters for the nonbonded van der Waals interactions. The OPLS parameters were chosen in order to obtain a consistent calculation when the OPLS model for chloroform was used. The charges for the cyclophane and the pyrene molecules were calculated using the semiempirical AM1²⁹ method, since this method delivered charges, which were very similar to the standard OPLS ones. All atoms were treated explicitly. The solvent was also explicitly treated using the SPC (Single Point Charge) model for water³⁰ and the OPLS parameters for chloroform.³¹

The system consisted of the solute, either free pyrene or complex **2**, plus 1021 solvent molecules (water or chloroform) in a truncated octahedral box. Periodic boundary conditions were applied.

Simulations were carried out at constant temperature (300 K) and constant pressure (1 atm) by coupling the system to a Berendsen thermostat and manostat.³² The relaxation time was set to 0.1 ps for the temperature and to 0.5 ps for the pressure. The Newton equations of motions were integrated with 2 fs time step. The cutoff radius for the nonbonded interactions was set to 1.4 nm and was applied to so-called charge groups of atoms, which are defined such that the total net charge is zero. All bond lengths were kept constant using the SHAKE³³ algorithm with a relative geometric tolerance of 10⁻⁴.

Free energy calculations were performed using the thermodynamic integration method. The scaling of the potential function was performed using a soft-core pathway. In eq 3 both α_C and α_{LJ} parameters were set to 0.5 and the exponent *n* of λ was set to 2.

Due to the soft-core scaling, it was observed that at the end of the simulations with an almost deleted pyrene molecule inside the cyclophane cavity, the guest could move through the cyclophane atoms, escaping from the cavity. In order to avoid the sampling of non-relevant configurations, an extra term in the form of a simple harmonic potential energy function as shown in eq 7 was added to the total potential energy function in the simulations of the complex, restraining in this way the available space for the pyrene molecule to the cyclophane cavity. The restraining potential energy function

$$U_{\text{restr}} = \sum_{i=1}^5 \sum_{j=1}^{N_{\text{pyr}}} \frac{1}{2} K (r_{ij} - r_{ij,\text{max}})^2 \quad (7)$$

was acting only if the pyrene left the cavity ($r_{ij} > r_{ij,\text{max}}$) and otherwise $U_{\text{restr}} = 0$. *K* represents the force constant of the harmonic potential energy and was set to 1500 kJ mol⁻¹ nm⁻². The first summation runs over five host atoms that were chosen as reference for the distance check and which define the cavity limits (the two nitrogens bridging the molecule on the top and on the bottom, and the three spiro carbon atoms connecting each

(28) Jorgensen, W. L.; Tirado-Rives, J. *J. Am. Chem. Soc.* **1988**, *110*, 1657–1666.

(29) Dewar, M. J. S.; Zoebisch, E. G.; Healy, E. F.; Stewart, J. J. P. *J. Am. Chem. Soc.* **1985**, *107*, 3902–3909.

(30) Berendsen, H. J. C.; Postma, J. P. M.; van Gunsteren, W. F.; Hermans, J. *Intermolecular Forces*; Pullman, B., Ed.; Reidel: Dordrecht, 1981; pp 331–342.

(31) Jorgensen, W. L.; Briggs, J. M.; Contreras, M. L. *J. Phys. Chem.* **1990**, *94*, 1683–1686.

(32) Berendsen, H. J. C.; Postma, J. P. M.; van Gunsteren, W. F.; DiNola, A.; Haak, J. R. *J. Chem. Phys.* **1984**, *81*, 3684–3690.

(33) Ryckaert, J. P.; Cicciotti, G.; Berendsen, H. J. C. *J. Comput. Phys.* **1977**, *23*, 327–341.

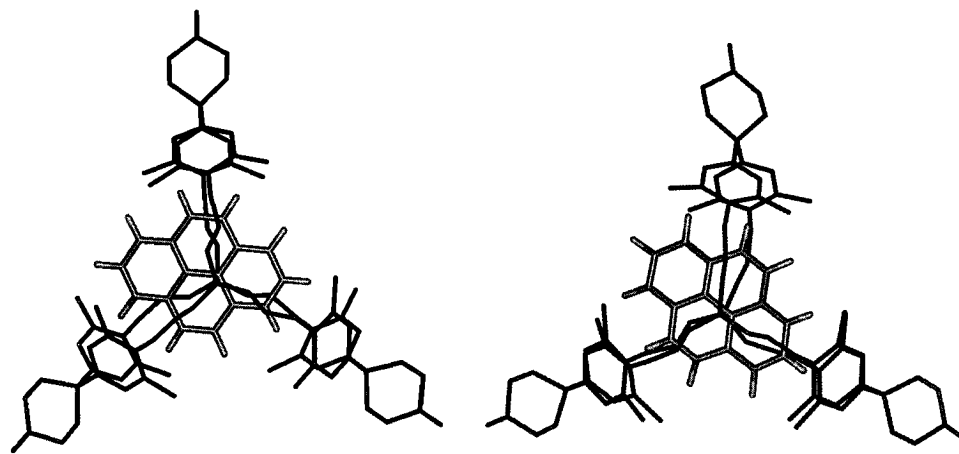


Figure 3. Top view of two isoenergetic conformations of the pyrene molecule in the cavity, which were found with a SPMC search.

two phenyl groups). The presence of the pyrene molecule inside the cavity was controlled using distances between these five atoms of the cyclophane molecule and all atoms of the pyrene molecule (N_{pyr}). r_{ij} represents the distance between one of the five reference cyclophane atoms and a pyrene atom. $r_{ij,\text{max}}$ is the maximum allowed distance between the reference atom i and a pyrene atom ($r_{ij,\text{max}} = 7.5 \text{ \AA}$ for the distances to the two nitrogen atoms and 12.5 \AA for the other distances to the three spiro carbon atoms).

Four simulation sets (two in water and two in chloroform) were carried out. The number of simulations for each set varied between 12 and 17, depending on the shape of the free energy curve. For each λ point on the free energy curve different simulation lengths were used, since they were carried out until a converged value was reached and the rate of convergence is different at different λ points. Especially in the λ region between 0.7 and 0.9 long simulations were needed, since large oscillations of the derivative of the energy were observed. The starting configurations at different λ points were obtained by gradually changing λ over 5 ps, allowing a smooth mutation of the system from one state to the next one. In total, the simulations for the deletion of the pyrene molecule in pure solvent required 575 ps for the water solution and 525 ps for the chloroform solution. The other two simulation sets for the deletion of the pyrene molecule inside the cyclophane cavity required 1270 ps in water and 1060 ps in chloroform.

5. Results and Discussion

The obtained curves of the free energy derivative for the four sets of simulations are shown in Figures 4A and 4B. Figure 4A shows the water simulations for deleting the pyrene molecule in the solvent box (solid line) and inside the cavity of the solvated cyclophane (dashed line). The curves for the same simulations, but in chloroform, are shown in Figure 4B. The integration of the curves obtained by fitting the points to a cubic spline delivers the Gibbs free energy corresponding to the process. This integration for the deletion of the pyrene molecule in pure water gave a Gibbs free energy value of $-49.1 \text{ kcal mol}^{-1}$, whereas the same deletion but inside the cavity of the cyclophane molecule in water yielded a Gibbs free energy contribution of $-31.5 \text{ kcal mol}^{-1}$. The difference of these two values, which corresponds, according to Scheme 1, to the Gibbs free energy of complexation in water ($\Delta G_1(\text{H}_2\text{O})$), is $-17.6 \text{ kcal mol}^{-1}$, whereas experimentally a value of $-9.4 \text{ kcal mol}^{-1}$ was measured.

The reliability of the methods and models used can be checked by looking at the hydration free energy for the pyrene molecule. This value can be calculated from the difference

between the deletion of pyrene in pure water ($-49.1 \text{ kcal mol}^{-1}$) and in the gas phase ($-53.2 \text{ kcal mol}^{-1}$). In this way the calculations deliver a free energy of hydration for pyrene of $-4.1 \text{ kcal mol}^{-1}$. Although an experimental value for pyrene is not available, the computed value of $-4.1 \text{ kcal mol}^{-1}$ compares well to the hydration free energy of similar molecules such as anthracene ($\Delta G_{\text{hydr}} = -4.3 \text{ kcal mol}^{-1}$) and phenanthrene ($\Delta G_{\text{hydr}} = -4.0 \text{ kcal mol}^{-1}$). The free energy of hydration for polycyclic aromatic molecules, such as anthracene, was calculated³⁴ with the same methodologies as those used in these calculations and showed a very good agreement with the experimental values. These results can therefore be considered as an indication of the accuracy at least of the model employed in the water simulations.

In chloroform the integral of the curves shown in Figure 4B was $-40.5 \text{ kcal mol}^{-1}$ for the annihilation of pyrene in pure solvent, whereas the deletion of pyrene in the cyclophane cavity gave $-33.1 \text{ kcal mol}^{-1}$. Here again the difference between these two values, $-7.4 \text{ kcal mol}^{-1}$, should correspond to the experimentally measured $-2.3 \text{ kcal mol}^{-1}$ for the complexation in chloroform.

The solvation free energy for pyrene in chloroform can also be calculated in a similar way as for the water simulations from the difference in free energy between the deletion of pyrene in pure chloroform ($-40.5 \text{ kcal mol}^{-1}$) and in the gas phase ($-53.2 \text{ kcal mol}^{-1}$). This procedure yields a free energy of solvation in chloroform for the pyrene molecule of $-12.7 \text{ kcal mol}^{-1}$. Unfortunately no experimental data for this process could be found. However, the value obtained is, as expected, larger than in the aqueous solution, since it involves the solvation of an apolar aromatic molecule by an aprotic solvent of low polarity, and is therefore plausible.

These results show a qualitative agreement of the calculated Gibbs free energies of complexation for the cyclophane–pyrene system in both water and chloroform solvents with the experimental ones. The trend of an energetically more advantageous complexation in water (polar solvent) than in chloroform (apolar solvent) was reproduced. Also the order of magnitude of the Gibbs free energy values corresponds to the experimental ones. However, in both cases it can be observed that the free energy of complexation is overestimated by the calculation. The difference in Gibbs free energy between the water and chloroform processes ($\Delta G_1(\text{CHCl}_3) - \Delta G_1(\text{H}_2\text{O}) = 10.2 \text{ kcal mol}^{-1}$) is closer to the experimental value ($7.1 \text{ kcal mol}^{-1}$) than the individual complexation free energies. This fact seems to point at a systematic error in the calculations, which thanks to the

(34) Mordasini Denti, T.; Beutler, T. C.; van Gunsteren, W. F.; Diederich, F. *J. Phys. Chem.* **1996**, *100*, 4256–4260.

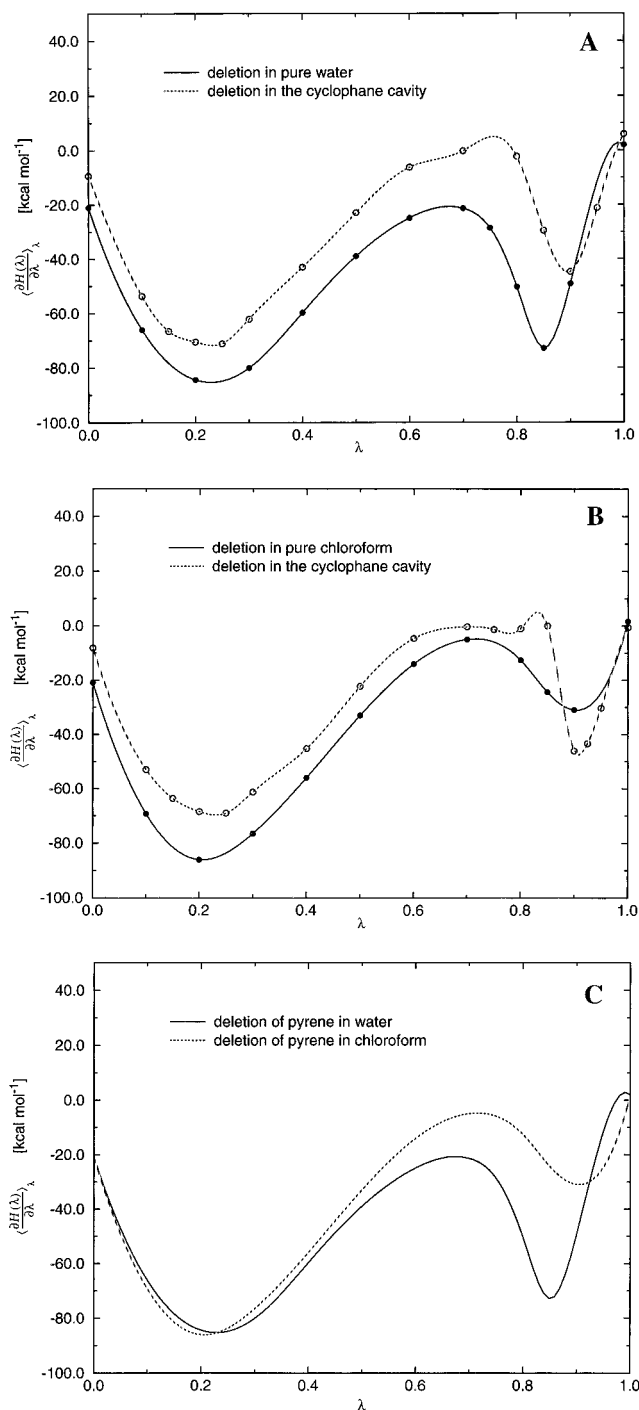


Figure 4. Derivative of the Gibbs free energy with respect to the coupling parameter λ , $\langle \partial H(\lambda) / \partial \lambda \rangle_\lambda$: (A) for the deletion of the pyrene molecule in a water box and inside the cavity of the cyclophane molecule, which is solvated with water; (B) for the deletion of the pyrene molecule in a chloroform box and inside the cavity of the cyclophane molecule, which is solvated with chloroform; and (C) for the deletion of the pyrene molecule in water (solid line) and chloroform (dashed line). All curves were fitted to the points using cubic splines.

last subtraction is cancelled out. The origin of this systematic error is not clear. One possibility is that the restraining interaction acting on the pyrene molecule during the deletion from the host restricts the entropy of the complex. This restriction is independent of the solvent in which the complexation occurs. This would explain why in a single thermodynamic cycle in water or chloroform the overestimation of the Gibbs free energy values is larger than for the difference in free energy of complexation between water and chloroform.

However, the value of the restraining energy term is very small in the various simulations, about 1 kcal mol^{-1} , if compared with the total nonbonded energies, which rules out a significant effect on the resulting ΔG values.

At $10.2 \text{ kcal mol}^{-1}$, the calculated value differs just $3.1 \text{ kcal mol}^{-1}$ from the experimental value ($7.1 \text{ kcal mol}^{-1}$). The result is satisfactory considering the factors that may cause a loss of accuracy: insufficient convergence of the ensemble averages for each λ point, use of a finite (12 to 17) number of λ values in the integration over λ , the subsequent subtraction (twice) of two comparable numbers, and last but not least force field inaccuracies.

A further analysis of the curves obtained from the deletion of the pyrene molecule inside the cyclophane cavity in water and chloroform (dashed lines in Figure 4A and 4B) reveals that they have in the λ region between 0.7 and 0.9 a less smooth character. A graphical analysis of the trajectories shows that exactly in this region solvent molecules attempt entering the cavity. This solvation of the cavity is possible because the guest has almost completely vanished at this point. At λ around 0.8, the van der Waals and electrostatic interactions between host and guest are scaled down to such an extent that they can no longer prevent the diffusion of the solvent into the cyclophane cavity. However, the deletion process is not yet totally completed (this will be the case when $\lambda = 1$), and the presence of the largely vanished guest molecule allows the solvent molecules to enter and leave the cavity. Depending on how many solvent molecules coexist with the largely vanished guest in the cavity, the energy of the system varies quite strongly. Very long simulations were needed in order to obtain a converged ensemble average. At $\lambda = 1$, when the pyrene is completely deleted, we could observe that the cyclophane cavity was occupied by ~ 8 solvent molecules, in the case of water, and by 2–3 solvent molecules in the case of chloroform. We can therefore conclude that the λ region between 0.7 and 0.9 is crucial to the accuracy of the calculation: for $\lambda < 0.7$ the presence of pyrene is still quite perceptible, whereas for $\lambda > 0.9$ the nonbonded host–guest interactions are too small to stop solvent molecules from diffusing into the space occupied by the pyrene molecule.

For the deletion of pyrene in pure water and in pure chloroform, the largest differences are also observed in the λ region between 0.7 and 0.9. Again the nonbonded interactions of pyrene are sufficiently scaled down allowing the penetration of the solvent molecules into the space previously occupied by the pyrene. The solvent molecules can then rebuild the interactions usually present in the bulk solvent. The strong cohesive interactions of water due to the complicated and extensive net of hydrogen bonds make the filling of the empty space more favorable in water than in chloroform, where weaker cohesive forces are present between the molecules. This fact is reflected in Figure 4C by the water curve lying below the chloroform curve. We can also consider the same effect from the opposite perspective: the free energies shown in Figure 4C approximately correspond, but with opposite sign, to the work needed for forming a cavity the size of the pyrene molecule (ΔG_{cav}) in the bulk solvent. This difference in free energy between the solvation of pyrene in water and chloroform was calculated to be $8.6 \text{ kcal mol}^{-1}$.

The free energy of complexation was divided into two terms: (i) guest–solvent interactions (ΔG_3 in Scheme 1), and (ii) host–guest and host–solvent interactions (ΔG_5 in Scheme 1). The calculations revealed that of these two terms, the first one (for the deletion of pyrene in pure solvent) represents the larger contribution to the total free energy of complexation. This

conclusion is valid for both the water and chloroform simulations. However, the work needed for creating a cavity (ΔG_{cav}) is larger in water than in chloroform. Therefore, when the pyrene is deleted, the free energy of cavitation is released ($-\Delta G_{\text{cav}}$), resulting in a total free energy of complexation more favorable in water than in chloroform.

The importance of this free energy of cavitation is evident when considering the calculation of the intrinsic complexation free energy for **2** in vacuo. The same thermodynamic cycle performed in solvent (Scheme 1) was carried out in vacuo. The calculations revealed that the free energy of complexation arising from just cyclophane and pyrene interactions and without any influence of solvent corresponds to $-19.9 \text{ kcal mol}^{-1}$. This strongly negative value clearly indicates that the pyrene molecule has very favorable interactions with the cyclophane cavity.

The separation of this (Gibbs) free energy term in the two components for the deletion of pyrene in vacuo and inside the cyclophane cavity also leads to interesting results. The disappearance of pyrene from the cyclophane cavity in vacuo corresponds almost exactly with the free energy change obtained for the same process in water ($-31.5 \text{ kcal mol}^{-1}$) and in chloroform ($-33.1 \text{ kcal mol}^{-1}$). We can therefore conclude that in the free energy change of this process the effect of the solvent is very small and that the obtained value is practically given just by cyclophane–pyrene interactions. In contrast, the free energy contribution arising from the deletion of the pyrene molecule in vacuo ($-53.2 \text{ kcal mol}^{-1}$) strongly differs from those obtained for the same process in water ($-49.1 \text{ kcal mol}^{-1}$) and in chloroform ($-40.5 \text{ kcal mol}^{-1}$). These results indicate that the pyrene molecule is stabilized by the interaction with water molecules by just $4.1 \text{ kcal mol}^{-1}$, whereas in chloroform this stabilization reaches $12.7 \text{ kcal mol}^{-1}$.

The key process which determines the solvent dependence for the cyclophane–pyrene complexation is therefore the elimination of pyrene molecules from the solvent and not directly the cyclophane–pyrene interactions, which are of similar magnitude in both solvents. From the total obtained ($10.2 \text{ kcal mol}^{-1}$) for the difference in complexation between water and chloroform solution, $8.6 \text{ kcal mol}^{-1}$ (about 84%) is caused by the differences in free energy of solvation of the pyrene molecule. These computational results fully support the hypothesis of Smithrud and Diederich,² which identified the internal cohesive interactions of the different solvents as a major factor controlling apolar binding strength. The importance of the free energy required for the formation of a cavity in pure solvent was also described by Blokzijl and Engberts³⁵ as a possible origin of the poor solubility of apolar molecules in water, reporting the solvation model of Lee.³⁶

The result that the free energy of cavitation gives a favorable contribution to the ΔG of complexation was also observed by Collet and co-workers,³⁷ when studying complexes of neutral molecules with cryptophane hosts. Sinanoglu³⁸ considered the free energy of cavitation as a “squeeze effect”, which can contribute in a more or less consistent way to the ΔG of complexation depending on the surface tension of the solvent. Since the surface tension is higher for the polar solvent water than for the apolar solvent chloroform, the ΔG_{cav} gained when deleting the guest molecule in pure solvent will be larger for water than for chloroform. Also Clarke *et al.*³⁹ studying

experimentally the inclusion complexes of cyclodextrin came to the conclusion that the large internal cohesion of water, which is due to hydrogen bonding, forces guest and host together. Örstan and Ross⁴⁰ observed that the addition of CaCl_2 to the water solution caused an increase in the surface tension and also an increase in the stability constant for the complexation of indole with cyclodextrin, whereas the addition of formamide, which decreases the surface tension of the solution, had the opposite effect and decreased the association constant. This experiment nicely showed the importance of the free energy of cavity formation in the bulk solvent and that solvent effects strongly depend on the free energy gain ($-\Delta G_{\text{cav}}$) when the guest is removed from the solvent and passes into the host cavity. All these experimental results are in agreement with the results of our calculations. Moreover, our conclusions that surface tension and cohesive forces play a major role in the preferred complexation for **2** in water are consistent with recent studies of ionophores at the water–chloroform interface performed by Wipff and Lauterbach.⁴¹

On the other hand, the complexation also requires that the solvent molecules which occupy the cyclophane cavity need to be removed and replaced by the pyrene molecule. The free energy term for these processes corresponds to $-\Delta G_5$ in Scheme 1. The desolvation of the cyclophane cavity is a free energy costing step; however, the favorable interactions between cyclophane and pyrene make the total process of complexation (desolvation of cyclophane cavity and subsequent penetration of the pyrene) not as unfavorable as would be the case if pyrene would have to create for itself a cavity in the bulk solvent. The presence of a preorganized cavity where pyrene can accommodate and experience more favorable interactions than in the bulk solvent explains the high association constant, which decreases if the cohesive interactions of the solvent also decrease. The free energy of water (for going from the liquid state to the ideal gas while keeping the total volume constant) at 298 K is $5.7 \text{ kcal mol}^{-1}$ (experimental⁴²) and is comparable to the free energy of $5.4 \text{ kcal mol}^{-1}$ calculated for the SPC water model,⁴² whereas the free energy for chloroform is only $3.7 \text{ kcal mol}^{-1}$ (experimental⁴³) and the calculated value for the chloroform model, obtained using the same computational procedure as in ref 43, is $3.4 \text{ kcal mol}^{-1}$.

The free energy required for the removal of the solvent from the cavity and replacing it with pyrene is slightly higher ($+33.1 \text{ kcal mol}^{-1}$) in chloroform than in water ($+31.5 \text{ kcal mol}^{-1}$). These results indicate that the chloroform molecules in the cyclophane cavity are involved in better interactions with the cyclophane than the water molecules. Diederich *et al.*⁵ reached the same conclusion observing that chloroform, benzene, and carbon disulfide seemed to interact favorably with the cyclophane cavity and therefore would act as weak competitive inhibitors. However, the precise free energy value $-\Delta G_5$ for this step is probably determined by an interplay of enthalpy and entropy, since the number of solvent molecules present in the cavity varies depending on their size.

6. Conclusions

Free energy calculations using the double annihilation technique were performed in water and chloroform, yielding

(39) Clarke, R. J.; Coates, J. H.; Lincoln, S. F. *Adv. Carb. Chem. Biochem.* **1988**, *46*, 205–249.

(40) Örstan, A.; Ross, A. *J. Phys. Chem.* **1987**, *91*, 2739–2745.

(41) Wipff, G.; Lauterbach, M. *Supramol. Chem.* **1995**, *6*, 187–207.

(42) Tironi, I. G.; Brunne, R. M.; van Gunsteren, W. F. *Chem. Phys. Lett.* In press.

(43) Tironi, I. G.; van Gunsteren, W. F. *Mol. Phys.* **1994**, *83*, 381–403.

(44) Reichardt, C. *Solvents and Solvent Effects in Organic Chemistry*, 2nd ed.; VCH: Weinheim, 1988; Chapter 7, pp 339–405.

(35) Blokzijl, W.; Engberts, J. B. F. *N. Angew. Chem.* **1993**, *105*, 1610–1648; *Angew. Chem., Int. Ed. Engl.* **1993**, *32*, 1545–1579.

(36) Lee, B. *Biopolymers* **1985**, *24*, 813–823.

(37) Canceill, J.; Lacombe, L.; Collet, A. *J. Am. Chem. Soc.* **1986**, *108*, 4230–4232.

(38) Sinanoglu, O. In *Molecular Interactions*; Ratajczak, H., Orville-Thomas, W. J., Eds.; John Wiley: Chichester, 1982; Vol. 3, pp 283–342.

the Gibbs free energy of complexation in the two solvents of different polarity. The free energy estimation was performed with the thermodynamic integration technique along a pathway which used a soft-core scaling of the nonbonded Lennard-Jones and Coulombic potential energy terms.

The calculated Gibbs free energy of complexation was -17.6 kcal mol⁻¹ in water and -7.4 kcal mol⁻¹ in chloroform. Both values are too large if compared with the experimental values of respectively -9.4 and -2.3 kcal mol⁻¹. However, they reproduce the more favorable complexation in water than in chloroform and are of the correct order of magnitude. The difference in free energy between the water and chloroform complexation could be reproduced more precisely: 10.2 kcal mol⁻¹ calculated compared with 7.1 kcal mol⁻¹ measured.

According to Scheme 1, the free energy of complexation was divided into two terms: (i) the deletion of the pyrene molecule in pure solvent (ΔG_3), and (ii) the desolvation of the cavity and the penetration of the pyrene molecule ($-\Delta G_5$). The analysis of these two terms in the complexation in water and chloroform revealed that the major contribution to the experimentally observed solvent effect is due to the removal of pyrene from the pure solvent (ΔG_3). This free energy value corresponds, but in the opposite direction, to the formation of a cavity the size of pyrene within the bulk solvent ($-\Delta G_{\text{cav}}$), also known as free energy of cavitation. The result obtained by computer simulation fully supports the conclusions of several previous experimental studies.³⁷⁻⁴⁰

The strong solvent effect on the association strength observed when changing the solvent from water to chloroform is therefore due to the difference in free energy of cavitation for the two solvents (8.6 kcal mol⁻¹), which, in return, is due to the differences in surface tension.

On the other hand, the favorable pyrene-cyclophane interactions also play an important role in the binding process, since

they contribute to compensate for the free energy needed for the desolvation of the cavity. The total free energy needed for the desolvation of the cyclophane cavity and subsequent pyrene complexation ($-\Delta G_5$ in Scheme 1) depends only slightly on the nature of the solvent ($+33.1$ kcal mol⁻¹ in chloroform and $+31.5$ kcal mol⁻¹ in water), indicating a small preference of the apolar cavity for being solvated with apolar chloroform rather than with polar water.

The desolvation of the cyclophane cavity is costly in terms of free energy. In water, a cluster of up to 8 solvent molecules needs to be removed in order to accommodate the guest, whereas in chloroform just 2-3 molecules occupy the cyclophane cavity. The necessary work for desolvation of the cavity and substitution of the solvent molecules by the pyrene is however very similar for both water and chloroform solvents, indicating an interplay of enthalpy and entropy. It is therefore the difference in free energy of cavitation for the two solvents that is the crucial term determining the strengths of association for pyrene and cyclophane.

The method described in this paper is quite expensive in terms of computational costs. However, thanks to the rapid evolution of the hardware capabilities, we are confident that the deletion of large molecules along a soft-core interaction pathway can soon become a standard method to compute host-guest binding free energies.

Acknowledgment. We thank Dr. Thomas C. Beutler for many suggestions and helpful discussions.

Supporting Information Available: AM1-derived charges used for all simulations of cyclophane-pyrene complex **2** (2 pages). Ordering information is given on any current masthead page.

JA960420H